Published in final edited form as:
Kidney Int. 2008 November ; 74(10): 1294–1309. doi:10.1038/ki.2008.394.

Dendritic cells facilitate accumulation of IL-17 T cells in the kidney following acute renal obstruction

Xiangyang Dong[1], **Lori A. Bachman**[1], **Melinda N. Miller**[1], **Karl A. Nath**[1], and **Matthew D. Griffin**[1]

[1] Division of Nephrology and Hypertension, Department of Medicine, Mayo Clinic College of Medicine, Rochester, Minnesota, USA

Abstract

Acute urinary obstruction causes interstitial inflammation with leukocyte accumulation and the secretion of soluble mediators. Here we show that unilateral ureteral ligation caused a progressive increase in renal F4/80$^+$ and F4/80$^-$ dendritic cells, monocytes, neutrophils and T-cells 24–72 h following obstruction. Depletion of dendritic cells by clodronate pretreatment showed these cells to be the most potent source of tumor necrosis factor and other pro-inflammatory mediators in the obstructed kidney. F4/80$^+$ dendritic cells and T-cells co-localized in the cortico-medullary junction and cortex of the obstructed kidney. Cytokine secretion patterns and surface phenotypes of T-cells from obstructed kidneys were found to include interferon-γ-secreting CD4$^+$ and CD8$^+$ memory T-cells as well as interleukin 17 (IL-17)-secreting CD4$^+$ memory T-cells. Depletion of the intra-renal dendritic cells prior to ligation did not numerically reduce T-cells in obstructed kidneys but attenuated interferon-γ and IL-17-competent T-cells. Our study shows that intra-renal dendritic cells are a previously unidentified early source of proinflammatory mediators after acute urinary obstruction and play a specific role in recruitment and activation of effector-memory T-cells including IL-17-secreting CD4$^+$ T-cells.

Keywords

obstructive nephropathy; inflammation; dendritic cells; T cells; tumor necrosis factor; interleukin 17

Localized inflammatory responses determine the extent and duration of renal dysfunction following acute kidney injury (AKI) because of ischemia, nephrotoxins, and urinary obstruction.[1–4] Persistence of intrarenal inflammation may foster irreversible interstitial fibrosis and chronic renal failure.[5] Insights into the cellular and molecular mediators of renal injury-induced inflammation will likely lead to improved strategies for the prevention or treatment of AKI.[1,6–12] Important basic elements of the inflammatory injury response of the kidney include the early secretion of tumor necrosis factor (TNF, also commonly referred to as TNFα) and other cytokines and chemokines[13–15] and the rapid interstitial accumulation of neutrophils, monocytes, and T cells.[16–20]

Aspects of these phenomena that continue to be intensively studied are the precise actions of individual mediators, the most significant cellular sources of each within the injured kidney, and the role played by specific parenchymal and bone marrow-derived cell types in renal

Correspondence: Matthew D. Griffin, Regenerative Medicine Institute (REMEDI), NCBES, Orbsen Building, National University of Ireland, Galway, Ireland. matthew.griffin@nuigalway.ie.

DISCLOSURE

The authors have no financial disclosure to make relevant to the subject matter of this study.

functional decline or recovery.[1,4,10,15,19–24] Recently, we and others have reported that dendritic cells (DCs), which are typically viewed as antigen-presenting cells with potent capacity for T-cell activation,[25,26] form an extensive network of bone marrow-derived cells resident within the renal interstitium[27–31] and serve as a major source of proinflammatory mediators within hours of renal ischemia reperfusion injury (IRI).[27] These findings raise questions regarding the participation of renal DCs (rDCs) in the response to other forms of AKI as well as the degree to which DC-derived inflammatory mediators orchestrate other nonresident leukocyte populations.

Urinary obstruction represents a form of AKI that is commonly encountered clinically and is readily reproduced in animal models. Despite its overtly simple mechanical basis, the pathophysiology of postobstructive renal functional decline is complex.[32–36] The responses that reportedly occur within minutes to hours in the renal parenchyma include profound changes in renal hemodynamics; localized secretion of TNF and other proinflammatory mediators; margination and interstitial migration of monocytes, neutrophils, T cells, and macrophages; induction of epithelial cell apoptosis; and stimulation of profibrogenic factors such as TGFβ1 and connective-tissue growth factor.[32–37] It has been well demonstrated that absence or blockade of individual proinflammatory mediators (for example TNF) or specific infiltrating cell populations (for example monocytes and T cells) may ameliorate widespread apoptosis and deposition of excess interstitial collagen.[34,38–44]

We posited that additional insight into the inflammatory nature of postobstructive AKI could be gleaned from a more extensive characterization of intrarenal bone marrow-derived cell populations in the mouse unilateral ureteral ligation (UUL) model. We demonstrate here that rDCs are a potent early source of proinflammatory cytokines and chemokines. We also find that acute obstruction is associated with influx of separate interferon-γ (IFNγ)- and interleukin (IL)-17-competent memory T-cell populations, and that rDCs appear to be necessary for intrarenal accumulation of these predifferentiated effector T cells.

RESULTS

Acute urinary obstruction is associated with accumulation of multiple CD45$^+$ cell populations

Unilateral ureteral ligation in adult mice was employed to compare bone marrow-derived cell populations within obstructed and nonobstructed kidneys at 24 and 72 h. Monocytes, F4/80$^+$ and F4/80$^-$ DCs, neutrophils, 'helper' (CD4$^+$) T cells, and 'cytotoxic' (CD8$^+$) T cells were identified and expressed as a proportion of the total cells by multicolor flow cytometry of kidney cell suspensions using the pan-leukocyte marker CD45 and a panel of cell type-specific markers (Figure 1a). As shown in Figure 1, total CD45$^+$ cells and each of the cell populations analyzed were proportionately increased in obstructed compared to non-obstructed kidneys at 24 h. With the exception of CD8$^+$ T cells, all cell types exhibited a further increase within obstructed kidneys at 72 h. The proportionate increase in these cell types following acute urinary obstruction was confirmed to be due to a true numerical increase by calculating total cell numbers for each subtype in non-obstructed and obstructed kidneys at 72 h (Supplementary Figure S1). The relative maturation of F4/80$^+$ and F4/80$^-$ DCs within obstructed kidneys was also examined at 24 and 72 h by quantifying staining intensity for major histocompatibility complex II and the co-stimulatory ligand CD86 (Figure 2). There was increased major histocompatibility complex II and CD86 expression on DCs from obstructed kidneys at 24 h that was more marked for F4/80$^+$ DCs but declined by 72 h. It was concluded that a 72 h period of acute urinary obstruction is associated with a rapid, progressive accumulation of multiple bone marrow-derived cell types including F4/80$^+$ DCs. The maturation response of F4/80$^+$ DCs, however, peaks during the first 24 h and mature DCs are less abundant at 72 h even when the total number of DCs is still increasing.

Dendritic cells are potent secretors of proinflammatory mediators following acute ureteric obstruction

Intracellular and multicolor surface staining was used to determine the predominant TNF-producing cells early after UUL. Figures 3a and b demonstrate a representative experiment in which the frequency of TNF^+ cells was increased 24 h after UUL within cells from obstructed kidneys. The TNF^+ cells were almost exclusively $CD45^+$ and were highly enriched (>50% in multiple experiments) for $F4/80^+$ DCs (Figure 3c). A proportion of $F4/80^+$ DCs from nonobstructed kidneys was also TNF^+ albeit with lower staining intensity indicating that intrarenal $F4/80^+$ DCs are readily triggered to express TNF and that this capacity is heightened following acute urinary obstruction. To confirm that increased expression of TNF was present before disruption and overnight culture of kidney cell populations, the relative expression of TNF-encoding mRNA was assayed by quantitative RT-PCR (qRT-PCR) in freshly dissected kidney tissue at 24 and 72 h following UUL. As shown in Figure 3d, mRNA was increased in obstructed compared to nonobstructed kidneys at both time points and was highest at 72 h postobstruction. In addition, mRNA for TNF was increased in the CD11c-enriched fraction (but not the remaining $CD45^+$ fractions) of kidney cell suspensions from obstructed compared to nonobstructed kidneys before placement in culture (Figure 3e). In experiments not shown here, CD11c-enriched fractions prepared by magnetic bead separation from kidneys obstructed for 24 h were shown, by enzyme-linked immunosorbent assay (ELISA) of supernatants, to be many times more potent than CD11c-depleted fractions in the secretion of TNF, IL-6, MCP-1, MIP-2, RANTES, and IP-10. Thus, we concluded that rDCs, particularly $F4/80^+$ rDCs, are a highly potent source of TNF and other proinflammatory mediators during the early postobstructive time period in the ULL model.

T cells progressively accumulate at the corticomedullary junction (CMJ) and cortex and are colocalized with $F4/80^+$ DCs following acute urinary obstruction

The localization of T cells and $F4/80^+$ DCs within obstructed and nonobstructed kidneys was examined by immunohistochemistry of formalin-fixed, paraffin-embedded kidney sections stained for CD3 or F4/80 at 24 and 72 h following left UUL (see Supplementary Figure S2 and S3 for examples of staining patterns). In nonobstructed kidneys, $F4/80^+$ cells demonstrated typical dendritic morphology, were localized to the interstitium, and were most prominent at the CMJ and superficial cortex. Following 24 h of obstruction the distribution and morphology of $F4/80^+$ cells were no different from nonobstructed kidneys. At 72 h, $F4/80^+$ cells remained localized to the CMJ and cortex but were larger and more numerous, particularly in the cortex. T cells were enumerated at the two time points in the medulla, CMJ, and cortex. As shown in Figure 4a, increased numbers of interstitial T cells were observed at the CMJ and cortex following 24 h of urinary obstruction. At 72 h, there were further increases in T-cell numbers at the CMJ and cortex in addition to a moderate increase in T-cell numbers within the medulla. Following 72 h of obstruction there were multiple clusters of interstitial $CD3^+$ T cells present. Correlation with sequential sections stained for $F4/80^+$ demonstrated that T-cell clusters at the CMJ and cortex coincided with areas of prominent F4/80 staining (Figure 4b). The results indicated that rather than undergoing redistribution the $F4/80^+$ DCs of obstructed kidneys remain concentrated at the CMJ and cortex where they become more prominent and co-cluster with accumulating populations of T cells.

Preadministration of clodronate-containing liposomes specifically diminishes $F4/80^+$ intra-rDC numbers and reduces proinflammatory mediators

We have observed that $F4/80^+$ rDCs are greatly diminished *in vivo* by clodronate-containing liposomes.[27] To study intrarenal T-cell function in the presence or absence of rDCs, groups of mice were treated with clodronate-containing or inert (phosphate-buffered saline, PBS) liposomes and were subjected to UUL. Obstructed and nonobstructed kidneys were examined

48 h later for F4/80$^+$ DCs, F4/80$^-$ DCs, monocytes, CD4$^+$ T cells, and CD8$^+$ T cells. As shown in Figure 5 (with representative examples in Supplementary Figure S3), clodronate markedly reduced F4/80$^+$ DCs in obstructed as well as nonobstructed kidneys and modestly reduced F4/80$^-$ DCs but did not prevent increases of monocytes, CD4$^+$ T cells, or CD8$^+$ T cells. In separate experiments, cell suspensions from obstructed and nonobstructed kidneys of mice pretreated with clodronate or PBS liposomes were cultured overnight and proinflammatory mediators were measured in culture supernatants. To examine the contribution of bone marrow-derived cells, samples were cultured with and without removal of CD45$^+$ cells (Figure 6). For both groups, cell suspensions from obstructed kidneys secreted higher amounts of TNF, IL-6, RANTES, MCP-1, MIP-2, and IP-10 compared to those from nonobstructed kidneys with most or all of the secretion being attributable to CD45$^+$ cells. ELISA results for obstructed kidney samples from the two groups demonstrated that secretion of all mediators was lower following rDC depletion. These results indicated that rDCs (particularly F4/80$^+$ rDCs) can be greatly reduced in number by clodronate in the UUL model without impairing the accumulation of T cells and that this results in substantial attenuation of the postobstructive production of proinflammatory mediators.

Acute urinary obstruction results in intrarenal accumulation of separate IFN*γ*- and IL-17-competent T cells that is prevented by DC depletion

Utilizing clodronate or PBS liposome administration, experiments were carried out to characterize cytokine profiles of T cells in acutely obstructed kidneys in the presence and absence of rDCs. Following 24 h of obstruction, unsorted or CD4-enriched kidney cells were cultured overnight with or without a low dose of T-cell stimulatory antibody (anti-CD3ε—2C11). Supernatants were assayed for IL-2, IFN*γ*, IL-17 (Figure 7), and IL-4 (not shown). Obstructed but not control kidneys of PBS liposome-treated mice were characterized by 2C11-inducible secretion of IL-2, IFN*γ*, and IL-17 that was detectable in unsorted as well as CD4-enriched cells. Despite the presence of comparable numbers of T cells in the obstructed kidneys of clodronate-treated animals (see Figure 5) there was little or no 2C11-inducible secretion of these cytokines by cells from this group of animals. No detectable IL-4 secretion was present under any conditions (data not shown). In a similar experiment carried out following 72 h of obstruction (Figure 8a), inducible IL-17 but not IFN*γ* remained diminished in unsorted cells from obstructed kidneys of clodronate-compared to PBS liposome-treated animals. In the case of CD4-enriched cell preparations, there was a persistent marked reduction in inducible secretion of IFN*γ* and IL-17. The possibility that the capacity of intrarenal T cells to produce IFN*γ* and IL-17 was induced only following a period of *in vitro* culture was ruled out in separate experiments in which freshly isolated CD4-enriched cells from nonobstructed and obstructed kidneys were subjected to qRT-PCR for mRNA encoding the two cytokines of interest. As shown in Figure 8b, there was marked increase in mRNA for both IFN*γ* and IL-17 in CD4-enriched cells from obstructed compared to nonobstructed kidneys at 72 h.

Using intracellular staining for IFN*γ* and IL-17 combined with surface staining for CD45 and CD4 of unstimulated and 2C11-stimulated kidney cells, it was shown that separate populations of CD4$^+$ IFN*γ*-competent (Th1) and CD4$^+$ IL-17-competent (Th17) T cells (as well as CD4$^-$ populations of each) were present within obstructed kidneys at 72 h (Figure 9a). It was also shown by qRT-PCR that expression of the primary activating cytokines for Th1 and Th17 T cells, IL-12 and IL-23, was increased in whole-kidney tissue as well as CD11c-enriched cell fractions following acute urinary obstruction (Figure 9b). It was concluded that acute urinary obstruction is associated with early accumulation of distinct Th1 and Th17 CD4$^+$ T-cell populations (in addition to CD4- T cells) that are competent to secrete high levels of IFN*γ* and IL-17 following brief, low-dose stimulation through the T-cell receptor. The presence or functional capacity of these differentiated T-cell populations was shown to be diminished by predepletion of intra-rDCs and likely to be dependent on DC-produced activating factors.

Intrarenal IFN*γ*- and IL-17-competent T cells in the acutely obstructed kidney have characteristics of memory T cells

Intrarenal IFNγ- and IL-17-competent T cells in obstructed kidneys were further characterized by flow cytometry. Kidney cells were enriched for $CD45^+$ cells and cultured overnight with varying doses of 2C11. IL-17^+ $CD4^+$ $CD44^{hi}$ cells and, to a lesser extent, IFNγ^+ $CD4^+$ $CD44^{hi}$ cells were detectable in preparations from obstructed kidneys at 72 h even in the absence of 2C11 stimulation with additional numbers detectable following as little as 0.001 μg/ml of 2C11 (Supplementary Figure S4). Separate analysis of $CD8^+$ T cells indicated the presence of 2C11-inducible IFNγ^+ $CD8^+$ $CD44^{hi}$ cells that were also responsive to very low concentration of 2C11 (see Supplementary Figure S4). Additional analyses indicated that the large majority of IL-17-competent T cells within obstructed kidneys were $CD4^+$, whereas IFNγ-competent cells consisted of separate $CD4^+$, $CD8^+$, and $CD4^-$/$CD8^-$ populations. In addition, small numbers of $CD4^+$/$CD8^+$ T cells were noted some of which stained for IFNγ or IL-17 (Supplementary Figure S5). The characteristics of these T-cell populations were suggestive of a predifferentiated memory phenotype and a staining panel of relevant surface markers was applied to further characterize them (Figure 10). This indicated that IL-17^+ $CD4^+$ T cells from obstructed kidneys were $CD44^{hi}$ $CD45RB^{lo}$ $CD62L^{lo}$ $CD69^+$, $CD25^+$—consistent with activated memory $CD4^+$ T cells. A smaller population of IL-17^+ $CD4^-$ cells were present and exhibited a similar staining profile. These cells did not stain for TCR$\gamma\delta$, NK1.1, or CD8. A separate analysis of IFNγ^+ cells yielded similar results with the exception that IFNγ^+ cells were not $CD45RB^{lo}$ and the majority of IFNγ^+ $CD4^-$ cells were $CD8^+$ (Supplementary Figure S6). An overall conclusion was reached that acute urinary obstruction results in intrarenal accumulation of memory-phenotype T-cell populations with distinct cytokine-secreting capacities including Th17- and Th1-type $CD4^+$ T cells, IFNγ-competent $CD8^+$ T cells, and lesser numbers of double-negative and double-positive T cells.

Dendritic cell depletion prevents accumulation of $CD44^{hi}$ T cells in the kidney following acute urinary obstruction

Although depletion of DCs before UUL did not prevent accumulation of T cells in the obstructed kidney, we postulated that the presence of rDCs may be necessary for recruitment or activation of memory-phenotype T cells. This was confirmed experimentally as shown in Figure 11. In groups of mice pretreated with clodronate or control liposomes and subjected to UUL, it was confirmed that following 72 h of obstruction there was marked reduction in $F4/80^+$ DCs but similarly increased numbers of $CD4^+$ and $CD8^+$ T cells in the obstructed kidneys of the clodronate-treated group. Nonetheless, although obstructed kidneys from the PBS group were characterized by increased proportions of $CD4^+$ and $CD8^+$ T cells that were $CD44^{hi}$ and by overall increase in mean fluorescence intensity for CD44 surface staining, there was no such alteration in CD44 staining in obstructed kidneys of mice in which $F4/80^+$ DCs numbers were reduced.

DISCUSSION

This study provides novel findings pertaining to the pathogenesis of obstruction-induced inflammation in three areas. First, acute urinary obstruction is associated with an early progressive increase in both $F4/80^+$ and $F4/80^-$ DCs in the kidney in addition to the previously reported infiltration by monocytes, neutrophils, and T cells. The cells in question can be clearly categorized as DCs rather than macrophages on the basis of morphology, surface and intracellular markers, maturation response, and T-cell stimulatory capacity.[27–31,45,46] Second, as we have recently reported for IRI,[27] rDCs constitute a potent source of proinflammatory mediators including TNF, IL-6, and MCP-1. In the case of TNF, we show here that the $F4/80^+$ rDC subset is the predominant secretor within 24 h of obstruction. Third, progressive accumulation of discrete $CD4^+$ and $CD8^+$ memory T cells that are predifferentiated for IFNγ

and IL-17 secretion is also a characteristic early feature of urinary obstruction. Although predepletion of rDCs does not prevent the postobstructive influx of T cells, it does reduce the presence of such predifferentiated effector memory T cells suggesting an *in situ* role for rDCs in arming phenotypically distinct effector memory T-cell responses to AKI.

Recent commentaries on the pathophysiology of obstructive uropathy highlight the well-established role of inflammation in early renal dysfunction and chronic fibrotic injury.[34,36] The most compelling evidence for this perspective was initially derived from histological studies demonstrating infiltration of leukocyte populations and expression analyses documenting increased presence of specific cytokines and chemokines in whole-kidney preparations.[34,47–50] More recently, genetically modified mouse strains and pathway-specific blocking agents have been applied to determine the role of individual molecular pathways in promoting cellular apoptosis and interstitial fibrosis.[34,36,39–43,51–53] Thus, we now know that TNF, MCP-1, TGFβ1, colony-stimulating factor 1, IL-6, and ligands for CCR1 and CCR2 exert nonredundant influences on postobstructive renal injury.[36,40–43] Although resident parenchymal renal cells and infiltrating bone marrow-derived leukocytes have the capacity to secrete and respond to these mediators,[22,54–56] infiltrating macrophages, which are typically identified in the mouse by staining with F4/80 or anti-CD68 antibodies, are frequently cited as the most significant early regulator of apoptosis, fibroblast activation, and epithelial to mesenchymal transformation.[34,51] Combined with previously published results characterizing rDCs in the healthy kidney,[27–31,46] our findings here indicate that the majority of F4/80$^+$ cells present in the kidney are DCs rather than macrophages. These interstitial F4/80$^+$ DCs, which also express other 'macrophage markers' including CD68, CD11b, and FcR, are present in relative abundance before the onset of obstruction.[27,28]

In contrast to IRI where we have observed constant DC numbers during the first 24 h,[27] F4/80$^+$ rDCs are increased following ureteral ligation at 24 and 72 h. In addition, we demonstrate a rapid response of these cells to the primary injury event in the form of DC maturation and production of TNF. Interestingly, immunohistochemical analysis indicates that F4/80$^+$ DCs remain most prominently localized to the CMJ and cortex throughout the first 72 h after onset of obstruction. Whether the subsequent decline in maturation level of these DCs between 24 and 72 h represents a shift in their pathogenic role now merits further investigation given the recent report of Scholz *et al*.[57] indicating an anti-inflammatory role of rDCs in nephrotoxic serum nephritis. The population of F4/80$^-$ DCs, which is relatively scant in the intact, disease-free kidney, increases substantially following acute obstruction—presumably being recruited from circulating immature DCs or representing DC differentiation of infiltrating monocytes. Although our experiments to date suggest a more active role for F4/80$^+$ DCs in early proinflammatory responses to obstruction, it will be necessary in the future to separately study the participation of F4/80$^-$ DCs in AKI. In general, we believe that previously unrecognized early abundance of rDCs rather than macrophages in the obstructed kidney represents an important shift in our understanding of the localized pathophysiology of injury in this disease model.

In this study, we also provide clear evidence for a plurality of differentiation phenotypes among accumulating T cells—most strikingly the Th1 and Th17 phenotypes present within the CD4$^+$ T-cell compartment and the IFNγ-secreting capacity of CD8$^+$ T cells. The expression by these cells of memory surface markers and the fact that high-level cytokine secretion is stimulated overnight by a low concentration of soluble anti-CD3 antibody indicate that these lymphocytes have undergone prior differentiation.[58] As effector memory T cells they are, therefore, primed for rapid response to antigen[59] and have the capacity to participate in the early stages of postobstructive AKI. Importantly, qRT-PCR studies demonstrate that increased expression of IFNγ and IL-17 among CD4-enriched cells of obstructed kidneys was present before placing the cells in culture and in the absence of additional T-cell receptor stimulation

indicating that the T-cell phenotypes we observed were not the result of *ex vivo* modifications. $CD4^+$ T cells have been implicated in the renal functional decline that occurs following AKI.[19,24,60,61] For example, depletion or blockade of $CD4^+$ T cells may ameliorate organ damage in models of IRI.[19,61,62] Despite these observations, current and available characterization of the phenotype and function of infiltrating T cells in AKI models is quite limited. Our finding of IFNγ-competent $CD4^+$ as well as $CD8^+$ T cells in obstructed but not control kidneys is, however, consistent with studies by Rabb and colleagues that have implicated IFNγ and the Th1 differentiation pathway in the adverse effects of T cells in renal IRI.[19,63]

The additional demonstration of $CD4^+$ T cells in the obstructed kidney that are armed to secrete IL-17 is of potentially high interest. This T-cell subtype, which has been dubbed Th17 or 'proinflammatory T cell', is now known to be present at sites of tissue-specific autoimmunity and to play a key pathogenic role.[64–67] As recently reviewed by Bettelli *et al.*,[66] Th17 T cells are known to have a complex dependency on soluble mediators. A variety of individual factors have been shown to be involved in the separate processes of differentiation, stabilization, and amplification of Th17 T cells including IL-6, TGFβ, IL-23, and IL-21.[66,67] During the differentiation process from naive T cells, the Th1 and Th17 phenotypes as well as regulatory T-cell populations may be mutually competitive based on the availability of such soluble mediators. In the case of predifferentiated effector memory T cells, however, our results would support a model whereby separate populations of Th1 and Th17 T cells coexist in the renal parenchyma and are activated for response by specific DC-produced cytokines including IL-12 and IL-23. Important questions regarding the timing of DC-mediated activation of effector memory T-cell populations following AKI, the role of soluble mediators produced by non-bone marrow-derived kidney cells in localized T-cell activation, and the pathogenic role of Th17 T cells in renal parenchymal injury and fibrosis remain to be addressed. Nonetheless, the current results and the emerging picture of this lymphocyte subset as a potent contributor to autoimmune and inflammatory diseases heighten the likelihood that they will be found have similar effects in the kidney.[64–67]

The strategy we have used to reduce rDCs has the advantage of being potent and quite selective as regards the major subsets of resident and infiltrating $CD45^+$ cells in the kidney. Specifically, we have not observed a deficit of monocyte or T-cell infiltration of the kidney despite administration of clodronate.[27] Nonetheless, the systemic nature of clodronate-induced depletion of phagocytic cells leaves open the possibility that absence or altered function of non-DC populations may be relevant to the observed results.[68,69] Although it is well documented that clodronate reversibly reduces circulating numbers of monocytes, monocyte repopulation (presumably from the bone marrow) appears to occur quite rapidly. In our experiments, ureteral ligation was carried out 48 h after the second of two clodronate liposome injections and organs were removed following an additional 24 or 48 h. We interpret our results as indicating that although depletion of $F4/80^+$ DCs remains virtually complete throughout this time period, monocyte repopulation occurs more rapidly and is accompanied by comparable renal infiltration to the control group. The application of more discretely targeted DC depletion models[57,70] may help to confirm the role of DCs in recruiting Th17 and other effector T cells to the kidney following obstruction. Finally, the antigen specificity and point of origin of the intrarenal memory T cells remain to be determined and, notably, a recent study demonstrates that interstitial $CD4^+$ T cells may be mobilized, following IRI, from both extrarenal and intrarenal pools.[71]

In summary, this study highlights the abundance and responsiveness of DCs during the early inflammatory response to urinary obstruction, reveals the diversity of potential T-cell effector functions in the obstructed kidney (including the recently described IL-17-secreting proinflammatory T cell), and introduces the possibility of a localized axis (DC–T cell) as a determinant of early tissue injury in this disease model.

MATERIALS AND METHODS

Experimental animals and reagents

Adult C57BL/6 (B6) mice were purchased from The Jackson Laboratory, Bar Harbor, ME and housed in a specific pathogen-free facility. All animal procedures were approved by the Institutional Animal Care and Use Committee. Tissue culture was carried out in Dulbecco's modified Eagle's medium supplemented with 10% FCS. A listing of detection agents, including clone numbers is provided as supplementary information on the Web.

Mouse model of unilateral ureteral ligation and preparation of kidney cell suspension

Unilateral ureteral ligation was carried out in adult mice under ketamine/xylazine anesthesia. A midline incision was made through the abdominal wall, the intestines were retracted, and the left ureter was identified. Two proline sutures were tied around the mid portion of the left ureter and the abdominal incision was closed in separate layers. Animals were observed for 2 h and killed between 24 and 72 h later. Kidneys were digested with collagenase and DNase as previously described.[31]

Flow cytometric analysis

Aliquots of cells were incubated in fluorescence-activated cell sorting buffer (PBS/0.2% bovine serum albumin/0.02%NaN_2) at 4 °C with combinations of fluorochrome-labeled and/or biotinylated antibodies followed by fluorochrome-labeled streptavidin. Intracellular staining of kidney cells was carried out using the Cytofix/Cytoperm kit (BD Pharmingen, San Diego, CA, USA). For experiments involving intracellular staining, suspensions were cultured overnight in Dulbecco's modified Eagle's medium/10% fetal calf serum with GolgiPlug (BD Pharmingen) added to 1 μl/ml 4 h before staining. For experiments involving T-cell stimulation, purified anti-CD3ε antibody (145-2C11) was added at the beginning of culture to concentrations varying between 0.001 and 1.0 μg/ml. Samples were analyzed using a FACS Calibur flow cytometer (BD Pharmingen) and WinMDI 2.8 software.

Clodronate liposome-mediated depletion of intrarenal DCs

Clodronate (Sigma-Aldrich, St Louis, MO, USA) and inert (PBS) liposomes were prepared as previously described.[27,68] Mice were injected intravenously with 200 μl of clodronate or PBS liposomes on 2 consecutive days then subjected to UUL 48 h after the second injection.

Magnetic column separation, cell culture, and ELISA of culture supernatants

Magnetic bead separations of kidney cell suspensions were carried out using antibody-coated microbeads and the miniMACS separation system (Miltenyi Biotech Inc., Auburn, CA, USA). Cultures of total cells and magnetic column cell fractions were carried out overnight in 96-well round-bottom plates following which supernatants were subjected to ELISA for TNF, IL-6, (BD Pharmingen), MCP-1, RANTES, MIP-2, and IP-10 (R&D Systems, Minneapolis, MN). For experiments comparing unsorted and CD45-depleted fractions or those comparing unsorted fractions from kidneys of clodronate-treated and control groups, cells were plated at 5×10^5 per well with 3–6 wells per condition. For experiments comparing CD4-enriched fractions from kidneys of clodronate-treated and control groups, cells were plated at 5×10^4 per well with 3–6 wells per condition.

Quantitative RT-PCR

Portions of freshly dissected kidneys were snap-frozen. The remaining portions were digested with collagenase and DNase followed by preparation of CD11c-enriched, CD11c-depleted/CD4-enriched, and CD11c-depleted/CD45-enriched fractions that were then pelleted and snap-frozen. Total RNA was extracted from all samples using PerfectPure Tissue and Cultured Cell

RNA (5 Prime, Gaithersburg, MD) kits and was reverse transcribed using the High-Capacity cDNA Archive kit (Applied Biosystems, Foster City, CA, USA). qRT-PCR was carried out in 96-well plates on selected samples for mouse TNF, IL-17, IFNγ, IL-12 p35, IL-23 p19, and glycer-aldehyde-3-phosphate dehydrogenase using inventoried TaqMan Gene Expression Assays, TaqMan Universal PCR Master Mix, and an ABI Prism 7900HT Real-Time System (Applied Biosystems). For all assays relative quantitation of gene expression was carried out by the comparative C_T method with amplification of glyceraldehyde-3-phosphate dehydrogenase as the reference. Comparative expression of a given target among samples was expressed as fold expression relative to a single control sample from nonobstructed kidney.

Immunohistochemistry and microscopic analysis

Freshly dissected kidneys were halved and fixed overnight at 4 °C in 10% formalin (Sigma-Aldrich) and were then embedded with paraffin. Sequential 6 μM sections were stained with primary antibodies against mouse CD3 (1:250) and F4/80 (1:200) using a Dako Autostainer (Dako, Carpinteria, CA, USA). Slides were deparaffinized and hydrated through an alcohol gradient. Peroxidase block and proteinase K were applied for 5 min each. Rodent block was applied for 30 min followed by primary antibody in Dako background-reducing diluent for 60 min. For anti-CD3 staining, MACH4 HRP Polymer (anti-rabbit secondary; Biocare Medical, Concord, CA, USA) was then applied for 30 min. For F4/80 staining, the Rat on Mouse secondary system was used (Biocare Medical). The rat probe was applied for 15 min, followed by the rat on mouse horseradish peroxidase polymer for 15 min. Betazoid DAB Chromogen (Biocare Medical) was then applied for 5 min. Slides were counterstained in hematoxylin, then dehydrated through an alcohol gradient and coverslipped. Stained slides were analyzed using a Nikon Eclipse E600 microscope with a Nikon DXM1200 digital camera. To quantify T cells in CD3-stained sections, positively stained cells were counted in a total of 10 nonoverlapping high-power (20 ×) fields in the medulla, at the CMJ, or in the cortex of each section. T-cell numbers at the three sites were expressed for each group as the mean±s.d. of the average counts from each kidney within the group.

Statistical analysis

Results for individual experimental groups were expressed as mean±s.d. and were compared using paired (for left vs right kidney experiments) or unpaired (for all other comparisons) two-sided Student's *t*-test with significance assigned to $P < 0.05$. Experiments were carried out between three and six times to ensure reproducibility.

Supplementary Material

Refer to Web version on PubMed Central for supplementary material.

Acknowledgments

The study was supported by NIH grants DK68545 (MDG) and D47060 (KAN).

References

1. Bonventre JV, Weinberg JM. Recent advances in the pathophysiology of ischemic acute renal failure. J Am Soc Nephrol 2003;14:2199–2210. [PubMed: 12874476]
2. Camussi G, Ronco C, Montrucchio G, et al. Role of soluble mediators in sepsis and renal failure. Kidney Int 1998;54(Suppl 66):S38–S42.
3. Sheridan AM, Bonventre JV. Cell biology and molecular mechanisms of injury in ischemic acute renal failure. Curr Opin Nephrol Hypertens 2000;9:427–434. [PubMed: 10926180]
4. Safirstein RL. Lessons learned from ischemic and cisplatin-induced nephrotoxicity in animals. Ren Fail 1999;21:359–364. [PubMed: 10416214]

5. Eddy AA. Progression in chronic kidney disease. Adv Chronic Kidney Dis 2005;12:353–365. [PubMed: 16198274]
6. Singri N, Ahya SN, Levin ML. Acute renal failure. JAMA 2003;289:747–751. [PubMed: 12585954]
7. Schrier RW, Wang W, Poole B, et al. Acute renal failure: definitions, diagnosis, pathogenesis, and therapy. J Clin Invest 2004;114:5–14. [PubMed: 15232604]
8. Liu KD. Molecular mechanisms of recovery from acute renal failure. Crit Care Med 2003;31(8 Suppl):S572–S581. [PubMed: 12907887]
9. Lameire N, Van Biesen W, Vanholder R. Acute renal failure. Lancet 2005;365:417–430. [PubMed: 15680458]
10. Day Y-J, Huang L, McDuffie MJ, et al. Renal protection from ischemia mediated by A2A adenosine receptors on bone marrow-derived cells. J Clin Invest 2003;112:883–891. [PubMed: 12975473]
11. Bellomo R, Bonventre J, Macias W, et al. Management of early acute renal failure: focus on post-injury prevention. Current Opin Crit Care 2005;11:542–547.
12. Han WK, Bonventre JV. Biologic markers for the early detection of acute kidney injury. Curr Opin Crit Care 2004;10:476–482. [PubMed: 15616389]
13. Takada M, Nadeau KC, Shaw GD, et al. The cytokine-adhesion molecule cascade in ischemia/reperfusion injury of the rat kidney. Inhibition by a soluble P-selectin ligand. J Clin Invest 1997;99:2682–2690. [PubMed: 9169498]
14. Ramesh G, Reeves WB. TNF-{alpha} mediates chemokine and cytokine expression and renal injury in cisplatin nephrotoxicity. J Clin Invest 2002;110:835–842. [PubMed: 12235115]
15. Patel NS, Chatterjee PK, Di Paola R, et al. Endogenous interleukin-6 enhances the renal injury, dysfunction, and inflammation caused by ischemia/reperfusion. J Pharmacol Exp Ther 2005;312:1170–1178. [PubMed: 15572648]
16. Ysebaert DK, De Greef KE, Vercauteren SR, et al. Identification and kinetics of leukocytes after severe ischaemia/reperfusion renal injury. Nephrol Dial Transplant 2000;15:1562–1574. [PubMed: 11007823]
17. Willinger CC, Schramek H, Pfaller K, et al. Tissue distribution of neutrophils in postischemic acute renal failure. Virchows Archiv B Cell Pathol 1992;62:237–243.
18. Klausner JM, Paterson IS, Goldman G, et al. Postischemic renal injury is mediated by neutrophils and leukotrienes. Am J Physiol 1989;256:F794–F802. [PubMed: 2541628]
19. Burne MJ, Daniels F, El Ghandour A, et al. Identification of the CD4(+) T cell as a major pathogenic factor in ischemic acute renal failure. J Clin Invest 2001;108:1283–1290. [PubMed: 11696572]
20. Boros P, Bromberg JS. New cellular and molecular immune pathways in ischemia/reperfusion injury. Am J Transplant 2006;6:652–658. [PubMed: 16539620]
21. Daemen MA, van't Veer C, Wolfs TG, et al. Ischemia/reperfusion-induced IFN-gamma up-regulation: involvement of IL-12 and IL-18. J Immunol 1999;162:5506–5510. [PubMed: 10228031]
22. Donnahoo KK, Meng X, Ao L, et al. Differential cellular immunolocalization of renal tumour necrosis factor-alpha production during ischaemia versus endotoxaemia. Immunology 2001;102:53–58. [PubMed: 11168637]
23. Miura M, Fu X, Zhang QW, et al. Neutralization of Gro alpha and macrophage inflammatory protein-2 attenuates renal ischemia/reperfusion injury. Am J Pathol 2001;159:2137–2145. [PubMed: 11733364]
24. Ysebaert DK, De Greef KE, De Beuf A, et al. T cells as mediators in renal ischemia/reperfusion injury. Kidney Int 2004;66:491–496. [PubMed: 15253695]
25. Banchereau J, Steinman RM. Dendritic cells and the control of immunity. Nature 1999;392:245–252. [PubMed: 9521319]
26. Steinman RM. The control of immunity and tolerance by dendritic cell. Pathol Biol 2003;51:59–60. [PubMed: 12801800]
27. Dong X, Swaminathan S, Bachman LA, et al. Resident dendritic cells are the predominant TNF-secreting cell in early renal ischemia-reperfusion injury. Kidney Int 2007;71:619–628. [PubMed: 17311071]

28. Kruger T, Benke D, Eitner F, et al. Identification and functional characterization of dendritic cells in the healthy murine kidney and in experimental glomerulonephritis. J Am Soc Nephrol 2004;15:613–621. [PubMed: 14978163]
29. Soos TJ, Sims TN, Barisoni L, et al. CX3CR1+ interstitial dendritic cells form a contiguous network throughout the entire kidney. Kidney Int 2006;70:591–596. [PubMed: 16760907]
30. Kaissling B, Le Hir M. Characterization and distribution of interstitial cell types in the renal cortex of rats. Kidney Int 1994;45:709–720. [PubMed: 8196273]
31. Dong X, Swaminathan S, Bachman LA, et al. Antigen presentation by dendritic cells in renal lymph nodes is linked to systemic and local injury to the kidney. Kidney Int 2005;68:1096–1108. [PubMed: 16105040]
32. Klahr S. Urinary tract obstruction. Semin Nephrol 2001;21:133–145. [PubMed: 11245776]
33. Chevalier RL. Pathogenesis of renal injury in obstructive uropathy. Curr Opin Pediatr 2006;18:153–160. [PubMed: 16601495]
34. Chevalier RL. Obstructive nephropathy: towards biomarker discovery and gene therapy. Nat Clin Pract Nephrol 2006;2:157–168. [PubMed: 16932414]
35. Vaughan J, Darracott E, Marion D, et al. Pathophysiology of unilateral ureteral obstruction: studies from Charlottesville to New York. J Urol 2004;172:2563–2569. [PubMed: 15538209]
36. Misseri R, Rink RC, Meldrum DR, et al. Inflammatory mediators and growth factors in obstructive renal injury. J Surg Res 2004;119:149–159. [PubMed: 15145697]
37. Misseri R, Meldrum KK. Mediators of fibrosis and apoptosis in obstructive uropathies. Curr Urol Rep 2005;6:140–145. [PubMed: 15717973]
38. Choi YJ, Baranowska-Daca E, Nguyen V, et al. Mechanism of chronic obstructive uropathy: increased expression of apoptosis-promoting molecules. Kidney Int 2000;58:1481–1491. [PubMed: 11012883]
39. Guo G, Morrissey J, McCracken R, et al. Role of TNFR1 and TNFR2 receptors in tubulointerstitial fibrosis of obstructive nephropathy. Am J Physiol 1999;277:F766–F772. [PubMed: 10564241]
40. Lenda DM, Kikawada E, Stanley ER, et al. Reduced macrophage recruitment, proliferation, and activation in colony-stimulating factor-1-deficient mice results in decreased tubular apoptosis during renal inflammation. J Immunol 2003;170:3254–3262. [PubMed: 12626584]
41. Meldrum KK, Metcalfe P, Leslie JA, et al. TNF-alpha neutralization decreases nuclear factor-kappaB activation and apoptosis during renal obstruction. J Surg Res 2006;131:182–188. [PubMed: 16412467]
42. Eis V, Luckow B, Vielhauer V, et al. Chemokine receptor CCR1 but not CCR5 mediates leukocyte recruitment and subsequent renal fibrosis after unilateral ureteral obstruction. J Am Soc Nephrol 2004;15:337–347. [PubMed: 14747380]
43. Wada T, Furuichi K, Sakai N, et al. Gene therapy via blockade of monocyte chemoattractant protein-1 for renal fibrosis. J Am Soc Nephrol 2004;15:940–948. [PubMed: 15034096]
44. Kluth DC, Erwig LP, Rees AJ. Multiple facets of macrophages in renal injury. Kidney Int 2004;66:542–557. [PubMed: 15253705]
45. Steiniger B, Klempnauer J, Wonigeit K. Phenotype and histological distribution of interstitial dendritic cells in the rat pancreas, liver, heart, and kidney. Transplantation 1984;38:169–174. [PubMed: 6380042]
46. Austyn JM, Hankins DF, Larsen CP, et al. Isolation and characterization of dendritic cells from mouse heart and kidney. J Immunol 1994;152:2401–2410. [PubMed: 8133051]
47. Schreiner GF, Harris KP, Purkerson ML, et al. Immunological aspects of acute ureteral obstruction: immune cell infiltrate in the kidney. Kidney Int 1988;34:487–493. [PubMed: 3264355]
48. Klahr S. Obstructive nephropathy. Internal Med 2000;39:355–361. [PubMed: 10830173]
49. Silverstein DM, Travis BR, Thornhill BA, et al. Altered expression of immune modulator and structural genes in neonatal unilateral ureteral obstruction. Kidney Int 2003;64:25–35. [PubMed: 12787392]
50. Crisman JM, Richards LL, Valach DP, et al. Chemokine expression in the obstructed kidney. Exp Nephrol 2001;9:241–248. [PubMed: 11423723]

51. Diamond JR, Kees-Folts D, Ding G, et al. Macrophages, monocyte chemoattractant peptide-1, and TGF-beta 1 in experimental hydronephrosis. Am J Physiol 1994;266:F926–F933. [PubMed: 7517644]
52. Zhang G, Kim H, Cai X, Lopez-Guisa JM, et al. Urokinase receptor deficiency accelerates renal fibrosis in obstructive nephropathy. J Am Soc Nephrol 2003;14:1254–1271. [PubMed: 12707394]
53. Yamagishi H, Yokoo T, Imasawa T, et al. Genetically modified bone marrow-derived vehicle cells site specifically deliver an anti-inflammatory cytokine to inflamed interstitium of obstructive nephropathy. J Immunol 2001;166:609–616. [PubMed: 11123344]
54. Frank J, Engler-Blum G, Rodemann HP, et al. Human renal tubular cells as a cytokine source: PDGF-B, GM-CSF and IL-6 mRNA expression *in vitro*. Exp Nephrol 1993;1:26–35. [PubMed: 8081949]
55. Prodjosudjadi W, Gerritsma JS, Klar-Mohamad N, et al. Production and cytokine-mediated regulation of monocyte chemoattractant protein-1 by human proximal tubular epithelial cells. Kidney Int 1995;48:1477–1486. [PubMed: 8544404]
56. Nee LE, McMorrow T, Campbell E, et al. TNF-alpha and IL-1beta-mediated regulation of MMP-9 and TIMP-1 in renal proximal tubular cells. Kidney Int 2004;66:1376–1386. [PubMed: 15458430]
57. Scholz J, Lukacs-Kornek V, Engel DR, et al. Renal dendritic cells stimulate IL-10 production and attenuate nephrotoxic nephritis. J Am Soc Nephrol 2008;19:527–537. [PubMed: 18235094]
58. Rogers PR, Dubey C, Swain SL. Qualitative changes accompany memory T cell generation: faster, more effective responses at lower doses of antigen. J Immunol 2000;164:2338–2346. [PubMed: 10679068]
59. Lanzavecchia A, Sallusto F. Understanding the generation and function of memory T cell subsets. Curr Opin Immunol 2005;17:326–332. [PubMed: 15886125]
60. De Greef KE, Ysebaert DK, Dauwe S, et al. Anti-B7-1 blocks mononuclear cell adherence in vasa recta after ischemia. Kidney Int 2001;60:1415–1427. [PubMed: 11576355]
61. Ascon DB, Lopez-Briones S, Liu M, et al. Phenotypic and functional characterization of kidney-infiltrating lymphocytes in renal ischemia reperfusion injury. J Immunol 2006;177:3380–3387. [PubMed: 16920979]
62. Zwacka RM, Zhang Y, Halldorson J, et al. CD4(+) T-lymphocytes mediate ischemia/reperfusion-induced inflammatory responses in mouse liver. J Clin Invest 1997;100:279–289. [PubMed: 9218504]
63. Yokota N, Burne-Taney M, Racusen L, et al. Contrasting roles for STAT4 and STAT6 signal transduction pathways in murine renal ischemia-reperfusion injury. Am J Physiol 2003;285:F319–F325.
64. Harrington LE, Mangan PR, Weaver CT. Expanding the effector CD4 T-cell repertoire: the Th17 lineage. Curr Opin Immunol 2006;18:349–356. [PubMed: 16616472]
65. Dong C. Diversification of T-helper-cell lineages: finding the family root of IL-17-producing cells. Nat Rev Immunol 2006;6:329–333. [PubMed: 16557264]
66. Bettelli E, Korn T, Kuchroo VK. Th17: the third member of the effector T cell trilogy. Curr Opin Immunol 2007;19:652–657. [PubMed: 17766098]
67. Veldhoen M, Hocking RJ, Atkins CJ, et al. TGFbeta in the context of an inflammatory cytokine milieu supports *de novo* differentiation of IL-17-producing T cells. Immunity 2006;24:179–189. [PubMed: 16473830]
68. Ciavarra RP, Taylor L, Greene AR, et al. Impact of macrophage and dendritic cell subset elimination on antiviral immunity, viral clearance and production of type 1 interferon. Virology 2005;342:177–189. [PubMed: 16143360]
69. Van Rooijen N, Sanders A. Liposome mediated depletion of macrophages: mechanism of action, preparation of liposomes and applications. J Immunol Methods 1994;174:83–93. [PubMed: 8083541]
70. Jung S, Unutmaz D, Wong P, et al. *In vivo* depletion of CD11c(+) dendritic cells abrogates priming of CD8(+) T cells by exogenous cell-associated antigens. Immunity 2002;17:211–220. [PubMed: 12196292]
71. Lai L-W, Yong K-C, Igarishi S, et al. A sphingosine-1-phosphate type 1 receptor agonist inhibits the early T-cell transient following renal ischemia-reperfusion injury. Kidney Int 2007;71:1223–1231. [PubMed: 17377506]

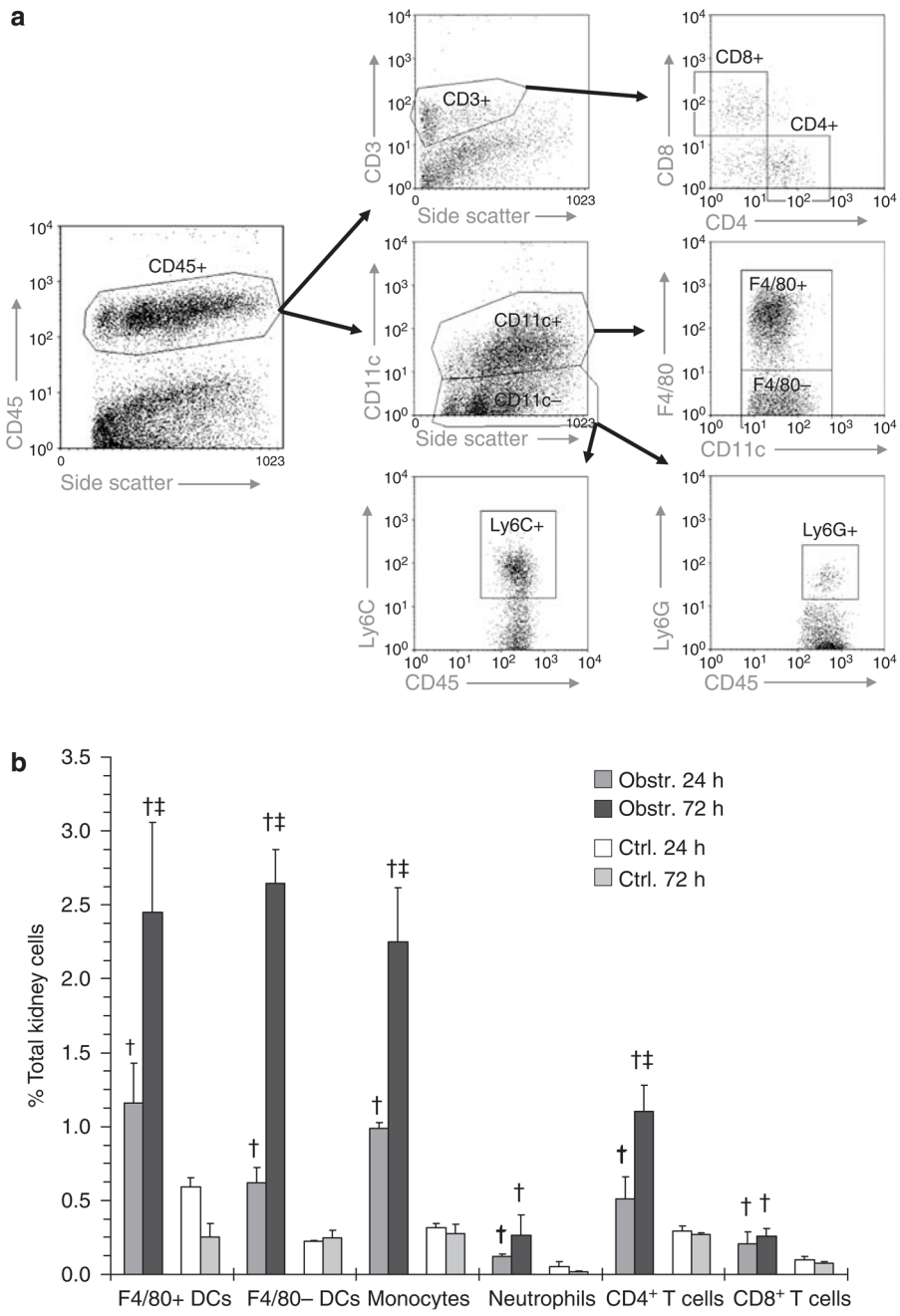

Figure 1. Progressive increase in multiple bone marrow-derived cell populations following acute renal obstruction

(**a**) Examples are shown of multicolor flow cytometry dot plots and gating used to analyze proportions of individual $CD45^+$ cell populations within total cell suspensions from collagenase/DNase-digested kidneys. The examples shown are from an obstructed kidney 72 h following ureteral ligation. Staining definitions for the individual cell populations were $F4/80^+$ DCs: $CD45^+/CD11c^+/F4/80^+/Ly6C^-$. $F4/80^-$ DCs: $CD45^+/CD11c^+/F4/80^-/Ly6C^-$. Monocytes: $CD45^+/Ly6C^+/CD11c^-$ (in separate experiments this population was also shown to be CD11b-hi). Neutrophils: $CD45^+/Ly6G^+/CD11c^-$. $CD4^+$ T cells: $CD45^+/CD3^+/CD4^+/CD8^-$. $CD8^+$ T cells: $CD45^+/CD3^+/CD8^+/CD4^-$. (**b**) The proportions of total kidney cells with

surface staining characteristics of F4/80$^+$ DCs, F4/80$^-$ DCs, monocytes, neutrophils, CD4$^+$ T cells, and CD8$^+$ T cells are shown graphically for obstructed (Obstr.) and nonobstructed (Ctrl.) kidneys from groups of mice (n = 3) killed at 24 and 72 h after unilateral (left) ureteral ligation. Each cell population is expressed as mean±s.d. of the percent of total kidney cells expressing the designated staining characteristics by multicolor flow cytometry. $^{\dagger}P<0.05$ for Obstr. vs Ctrl. at the same time point. $^{\ddagger}P<0.05$ for 72 vs 24 h. The difference in F4/80$^+$ DCs between control kidneys at 24 and 72 h has not been a reproducible finding.

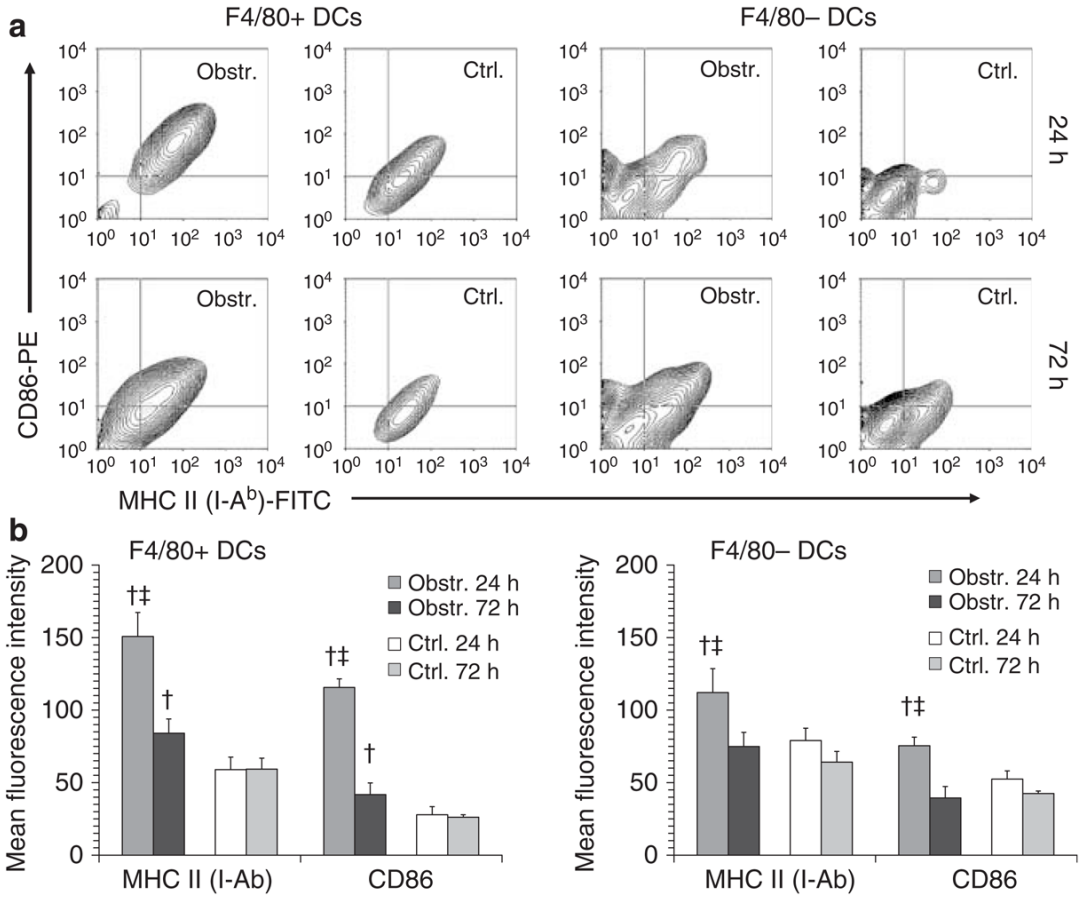

Figure 2. Increased maturation marker expression by DCs in acutely obstructed kidneys

(**a**) Examples are shown of flow cytometry contour plots indicating MHC II (I-A^b) and CD86 (B7-2) surface staining of F4/80$^+$ DCs (left) and F4/80$^-$ DCs (right). For both DC populations, initial gating was performed on cells staining positive for CD45 and for the DC-specific marker CD11c. Dot plots are shown for cells derived from obstructed (Obstr.) and nonobstructed (Ctrl.) kidneys at 24 and 72 h following unilateral (left) ureteral ligation. (**b**) Results are presented graphically for groups of three mice each killed at 24 and 72 h following unilateral ureteral ligation. Surface staining levels of MHC II and CD86 on F4/80$^+$ DCs (left) and F4/80$^-$ DCs (right) are expressed as mean±s.d. of the mean fluorescence intensity by flow cytometric analysis. $^{\dagger}P<0.05$ for Obstr. vs Ctrl. at the same time point. $^{\ddagger}P<0.05$ for 24 vs 72 h.

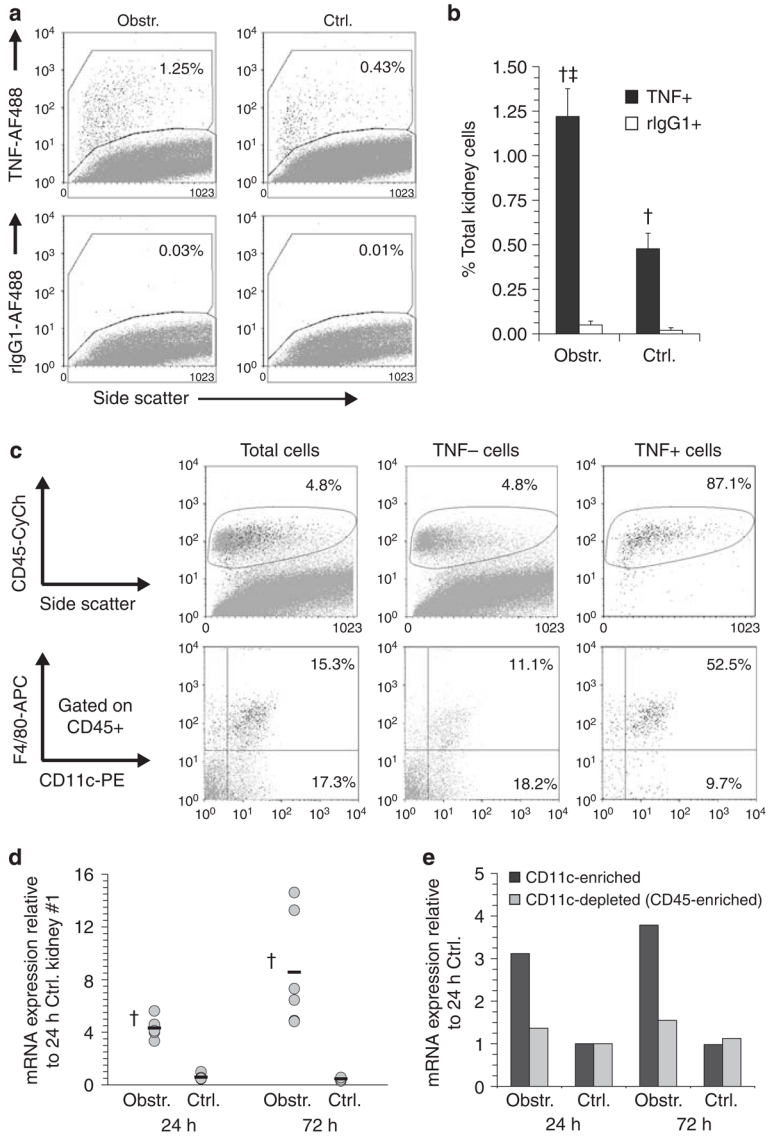

Figure 3. F4/80$^+$ DCs are the predominant TNF-producing cell early following acute renal obstruction

(**a**) Examples of flow cytometric dot plots of cell suspensions from obstructed (Obstr.) and nonobstructed (Ctrl.) kidneys stained intracellularly with a monoclonal antibody against TNF (TNF-AF488, upper plots) or with an isotype control antibody (rIgG1-AF488). Staining was carried out 24 h following unilateral (left) ureteral ligation. The percent of the total cells within the positive staining region are indicated. (**b**) Graphical results are shown for intracellular staining of cell suspensions from a total of four pairs of obstructed (Obstr.) and nonobstructed (Ctrl.) kidneys. Staining was carried out 24 h following unilateral ureteral ligation. Results are expressed as mean±s.d. percent total kidney cells staining positive with anti-TNF (TNF$^+$) or isotype control (rIgG1$^+$) antibodies as measured by flow cytometry. $^{\dagger}P<0.05$ for anti-TNF vs isotype control. $^{\ddagger}P<0.05$ for Obstr. vs Ctrl. (**c**) Examples are shown of multicolor flow cytometric analysis of total kidney cells, TNF-negative (TNF$^-$) and TNF-positive (TNF$^+$) cells 24 h following ureteral ligation. Intracellular staining and gating for TNF$^+$ and TNF$^-$ cells was carried out as illustrated in (**a**). Staining of each population for CD45 is shown in the upper plots with the percentage of the cells contained within the positively stained region indicated.

Staining of $CD45^+$ cells from each population for CD11c and F4/80 is shown in the lower plots. The percentages of the cells that are $CD11c^+/F4/80^+$ (i.e. $F4/80^+$ DCs) and $CD11c^+/F4/80^-$ (i.e. $F4/80^-$ DCs) are indicated. (**d**) Results of qRT-PCR for mRNA-encoding TNF are shown for individual obstructed and nonobstructed (Ctrl.) kidneys (gray circles) and for the means of each group (black bars, $n = 6$) at 24 and 72 h after left UUL. RNA was prepared without prior tissue digestion or culture. Results are expressed as fold expression relative to that of the first of six nonobstructed 24 h kidneys. $^{\dagger}P<0.05$ for Obstr. vs Ctrl. (**e**) Results are shown of qRT-PCR for mRNA-encoding TNF in pooled CD11c-enriched cells and CD11c-depleted, CD45-enriched cells from obstructed and nonobstructed kidneys at 24 and 72 h after left UUL. RNA was prepared without overnight culture. Results are expressed as fold expression relative to that of the cell preparations from the nonobstructed 24 h kidneys.

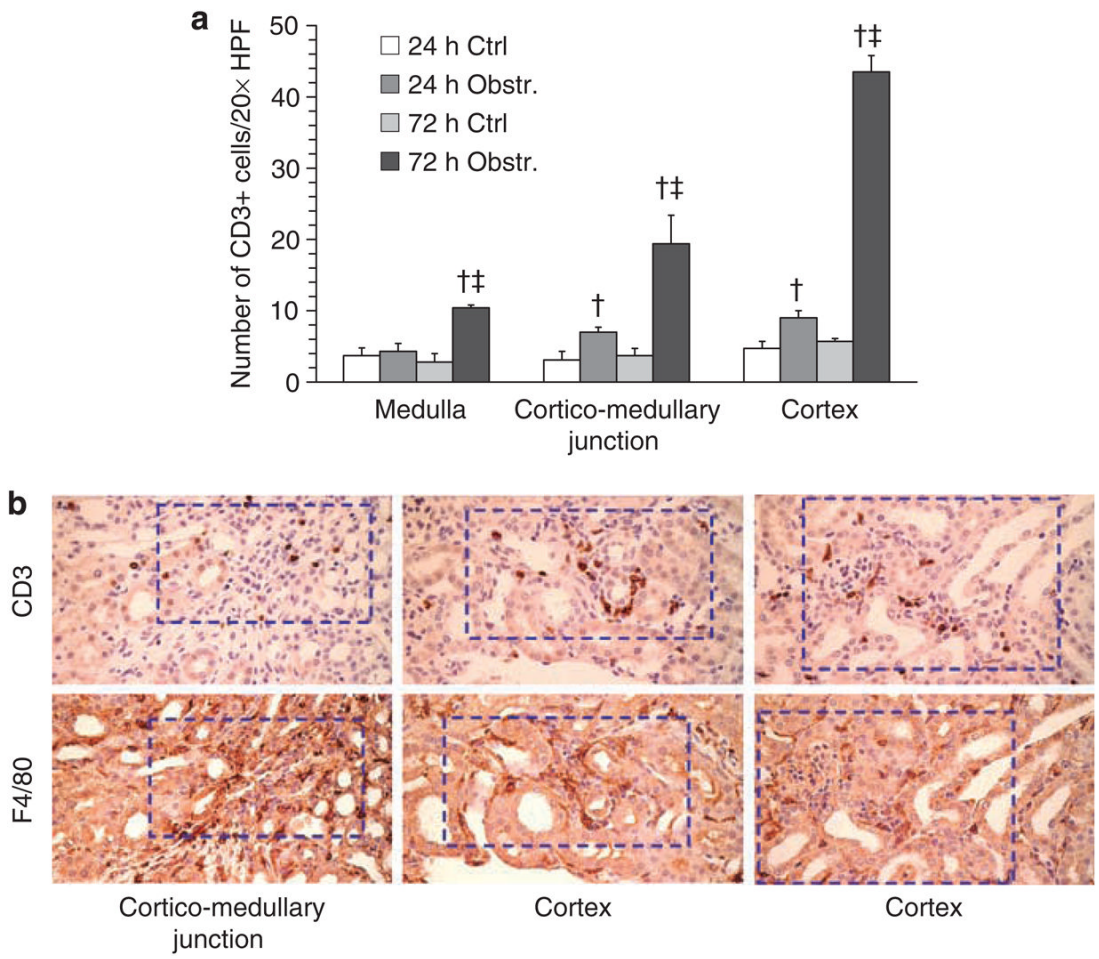

Figure 4. T cells accumulate at the corticomedullary junction and cortex following acute urinary obstruction and colocalize with F4/80$^+$ DCs

(**a**) Graphical results are shown for CD3$^+$ T cells numbers in immunostained sections of nonobstructed (Ctrl.) and obstructed (Obstr.) kidneys at 24 and 72 h after left UUL (n = 4 of each). Results are expressed as mean±s.d. of the total CD3$^+$ cells per high-power field in the medulla, corticomedullary junction, and cortex of each group. For each kidney, cells were counted and averaged from a total of 10 high-powered fields. $^{\dagger}P<0.05$ for Obstr. vs Ctrl.; $^{\ddagger}P<0.05$ for 72 vs 24 h. (b) Examples are shown of sequential sections of 72 h obstructed kidneys immunostained for CD3 (upper panels) and F4/80 (lower panels). Representative regions of the corticomedullary junction (left panels) and cortex (middle and right panels) containing clustered positively staining cells are indicated for each example by a dashed box.

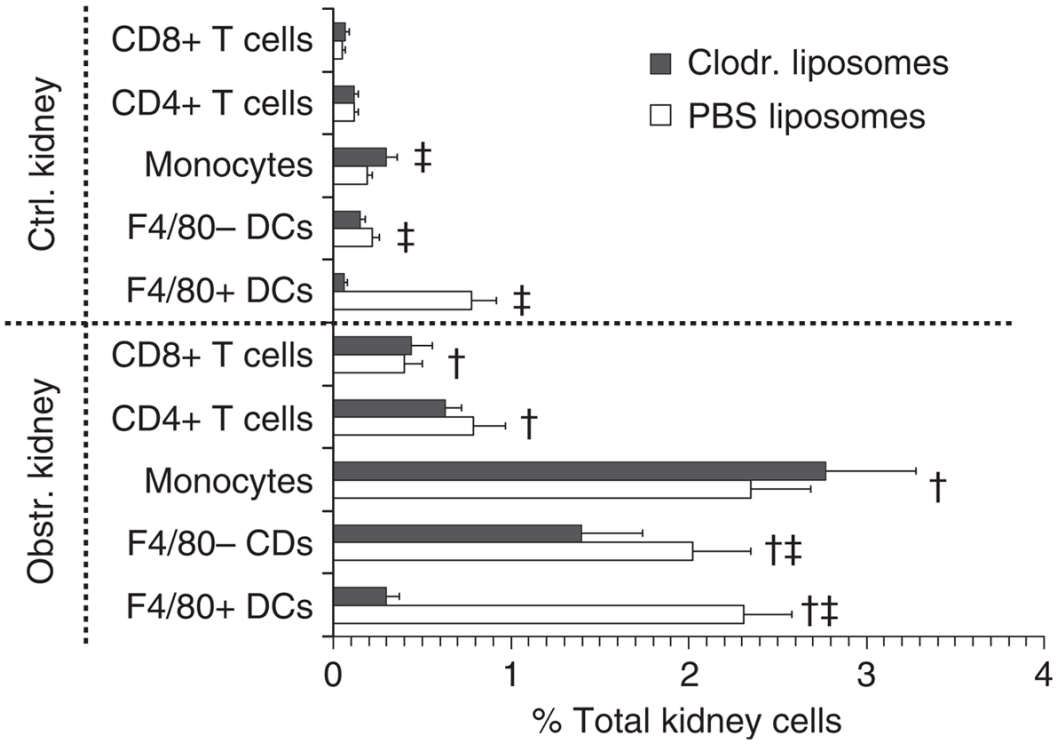

Figure 5. Clodronate-containing liposomes selectively reduce F4/80$^+$ DCs but do not prevent increased renal monocytes and T cells following acute renal obstruction

The proportions of total kidney cells with surface staining characteristics of F4/80$^+$ DCs, F4/80$^-$ DCs, monocytes, CD4$^+$ T cells, and CD8$^+$ T cells are shown graphically for obstructed (Obstr.) and nonobstructed (Ctrl.) kidneys from groups of mice pretreated with either clodronate-containing (Clodr.) or inert (PBS) liposomes (n = 5 each) and killed 48 h after unilateral (left) ureteral ligation. Each cell population is expressed as mean±s.d. of the percent of total kidney cells expressing the designated staining characteristics by multicolor flow cytometry. $^‡P<0.05$ for Clodr. vs PBS liposome groups. $^†P<0.05$ for Obstr. vs Ctrl. kidneys (for examples of dot plots for each cell type see Supplementary Figure S3).

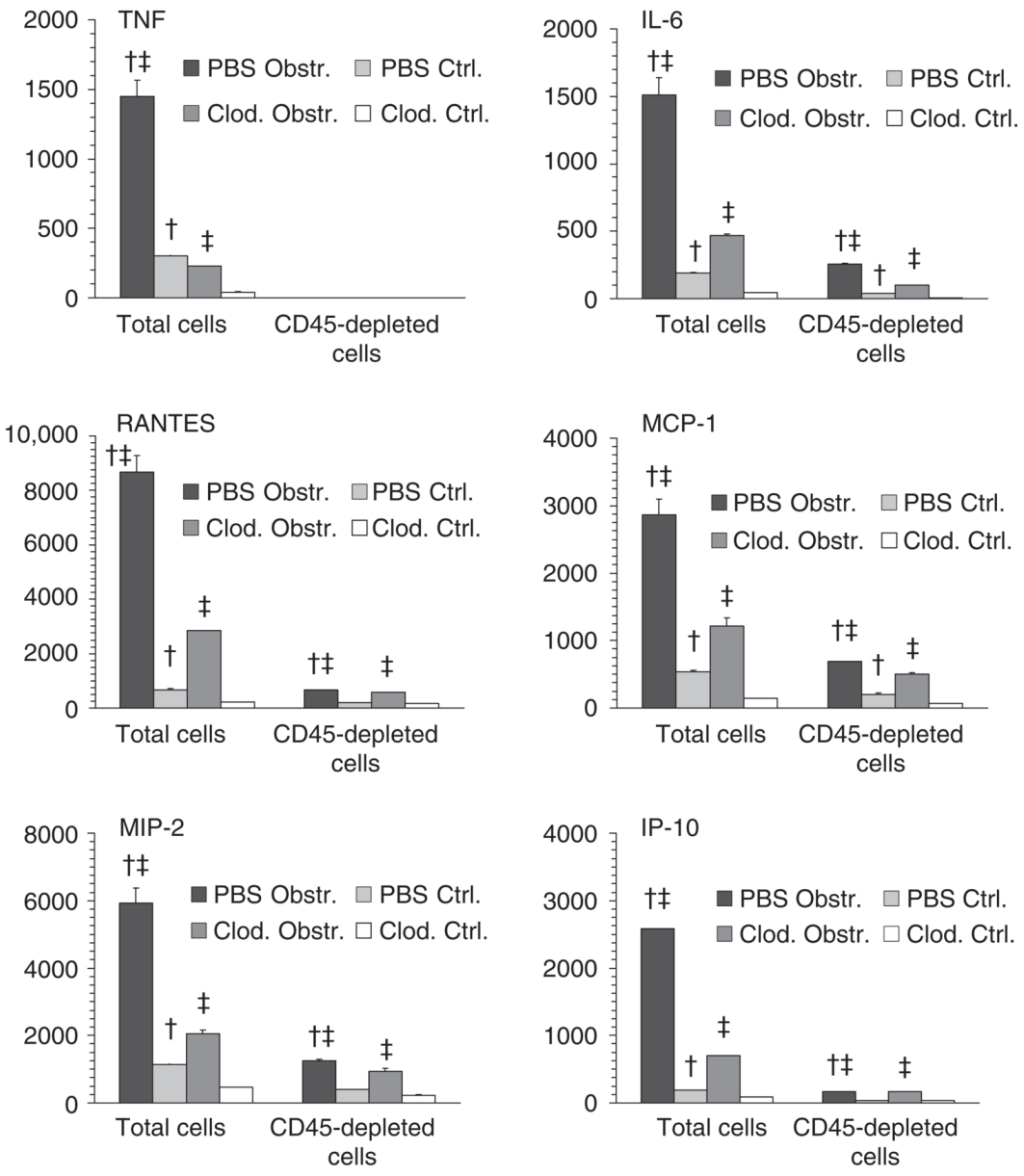

Figure 6. Renal DCs are required for maximal secretion of multiple proinflammatory mediators by bone marrow-derived cell populations within the acutely obstructed kidney

Graphical results are shown for multiple ELISAs of supernatants from overnight cultures of equal numbers of total kidney cells and CD45-depleted kidney cells derived from the obstructed (Obstr.) and nonobstructed (Ctrl.) kidneys of two groups of mice subjected 24 h previously to unilateral (left) ureteral ligation. The groups (n = 4 each) consisted of mice pretreated with either clodronate-containing (Clodr.) or inert (PBS) liposomes. All results are expressed as mean±s.d. concentration (pg/ml) of the proinflammatory mediator concentration in supernatants from each group of kidney cell cultures. ELISAs were carried out for TNF, IL-6, RANTES (CCL5), MCP-1 (CCL2), MIP-2 (CXCL2), and IP-10 (CXCL10). $^{\dagger}P<0.05$ for Clodr. vs PBS liposome groups. $^{\ddagger}P<0.05$ for Obstr. vs Ctrl. kidneys.

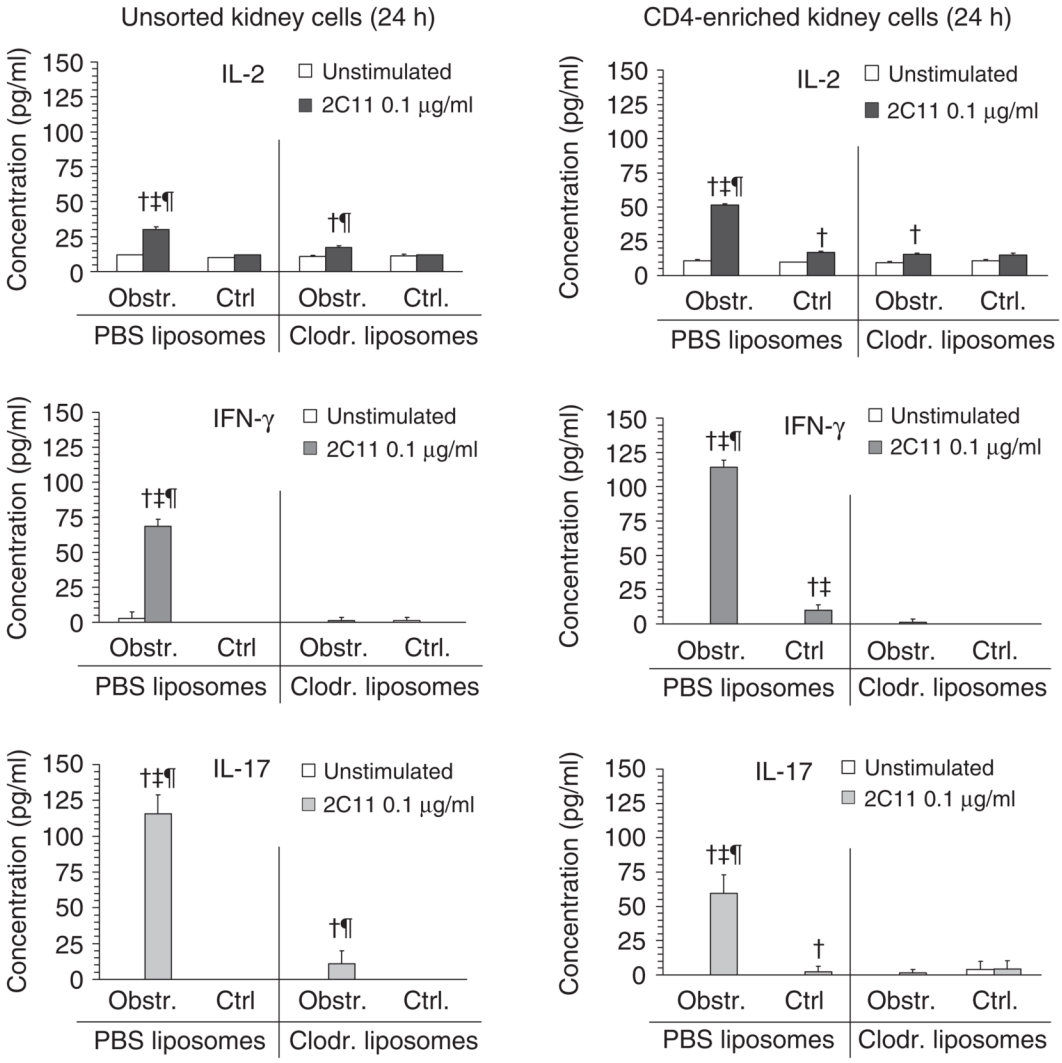

Figure 7. The presence of IFNγ- and IL-17-competent T cells in acutely obstructed kidneys is reduced by depletion of intrarenal DCs

Graphical results are shown for ELISAs of culture supernatants of cell suspensions from obstructed (Obstr.) and nonobstructed (Ctrl.) kidneys of groups of mice that were pretreated with inert (PBS) liposomes or clodronate-containing (Clodr.) liposomes (n = 3 of each). Cells suspensions were prepared 24 h following unilateral (left) ureteral ligation and plated in equal numbers for each condition in the absence (unstimulated) or presence (2C11 0.1 μg/ml) of a low amount of soluble anti-CD3 T-cell stimulatory antibody. Results, expressed as mean±s.d. of the concentration (pg/ml) of either IL-2, IFNγ, or IL-17 for each condition, are shown for total kidney cell suspensions (left graphs, unsorted kidney cells) and for CD4-enriched kidney cells (right graphs). $^{\dagger}P<0.05$ for 2C11 vs equivalent condition unstimulated. $^{\ddagger}P<0.05$ for PBS vs equivalent condition for Clodr. $^{\P}P<0.05$ for Obstr. vs equivalent Ctrl. kidney.

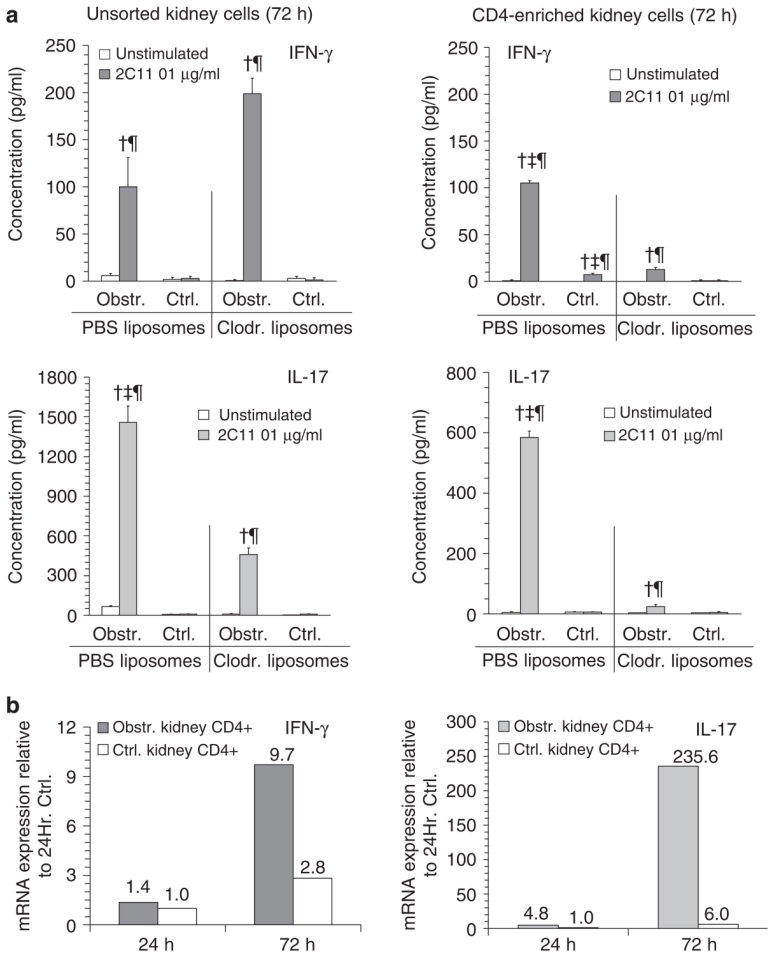

Figure 8. IL-17- and IFNγ-producing CD4$^+$ T-cell populations are increased in the kidney 72 h following acute urinary obstruction in the presence of DCs

(**a**) Graphical results are shown for ELISAs of culture supernatants of cell suspensions from obstructed (Obstr.) and nonobstructed (Ctrl.) kidneys of groups of mice that were pretreated with inert (PBS) liposomes or clodronate-containing (Clodr.) liposomes (n = 3 of each). Cell suspensions were prepared 72 h following unilateral (left) ureteral ligation and plated in equal numbers for each condition in the absence (unstimulated) or presence (2C11 0.1 μg/ml) of a low dose of soluble anti-CD3 T-cell stimulatory antibody. Results, expressed as mean±s.d. of the concentration (pg/ml) of either IFNγ or IL-17 for each condition, are shown for total kidney cell suspensions (left graphs, unsorted kidney cells) and for CD4-enriched kidney cells (right graphs). $^{\dagger}P<0.05$ for 2C11 vs equivalent condition unstimulated. $^{\ddagger}P<0.05$ for PBS vs equivalent condition for Clodr. $^{\P}P<0.05$ for Obstr. vs equivalent Ctrl. kidney. (b) Graphical results are shown for qRT-PCR assays of mRNA-encoding IFNγ (left graph) and IL-17 (right graph) in samples prepared from CD4-enriched cells of nonobstructed (Ctrl.) and obstructed kidneys of otherwise untreated mice at 24 and 72 h following left UUL. Cell samples were neither stimulated nor placed in culture before RNA extraction. Results are expressed as fold expression compared to the 24 h control sample with the numerical value for each column indicated above it.

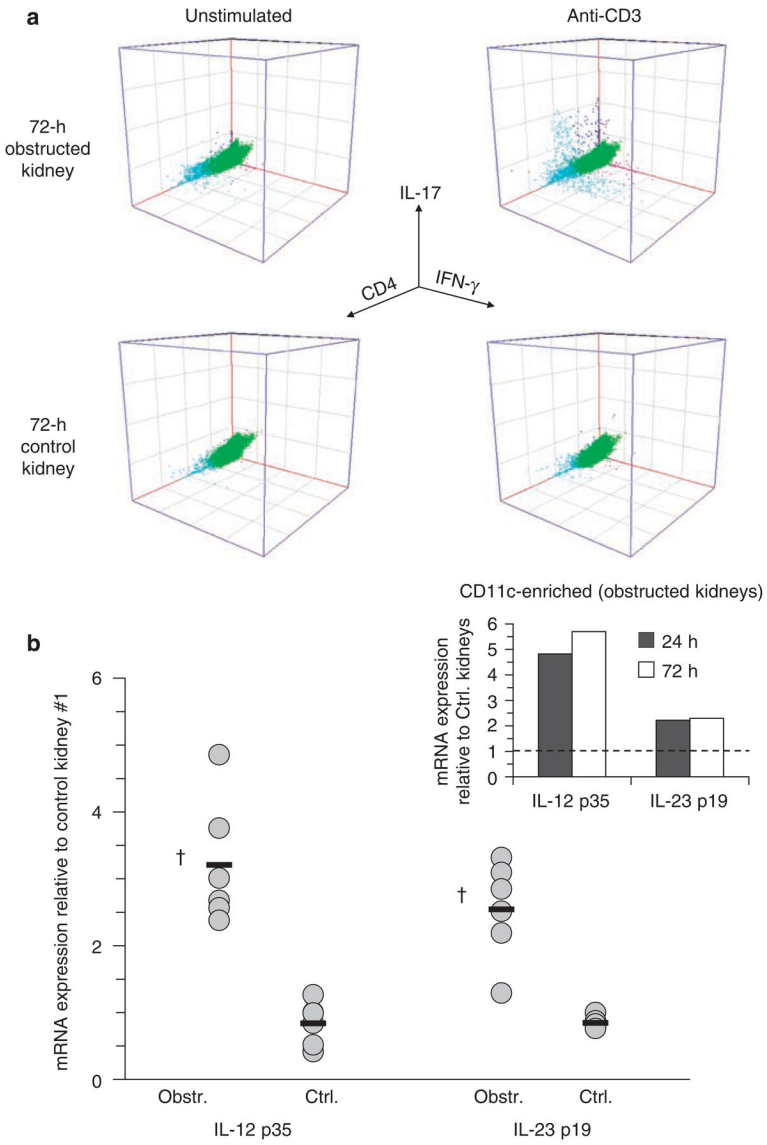

Figure 9. IFNγ and IL-17-competent T cells constitute separate cell populations within obstructed kidneys and are associated with early increased expression of DC-derived activating cytokines

(**a**) Examples of 3D flow cytometric dot plots are shown for kidney cell suspensions prepared from obstructed and nonobstructed (control) kidneys of normal adult mice 72 h following unilateral (left) ureteral ligation. Cell suspensions were cultured overnight with Golgi export inhibitor in the absence (unstimulated) or presence (anti-CD3) of soluble T-cell stimulatory antibody and then were surface stained for CD45 and CD4 and intracellularly stained for IFNγ and IL-17. Dot plots are gated on $CD45^+$ cells. Separate IFNγ and $IL\text{-}17^+$ populations that are predominantly (but not exclusively) $CD4^+$ are evident in the cell sample from obstructed kidney following anti-CD3 stimulation (right upper dot plot). (**b**) Results of qRT-PCR for mRNA-encoding the cytokine-specific chains for IL-12 (p35) and IL-23 (p19) are shown for individual obstructed and nonobstructed (Ctrl.) kidneys (gray circles, $n = 6$ of each) and for the means of each group (black bars) at 24 after left UUL. RNA was prepared without prior tissue digestion or culture. Results are expressed as fold expression relative to that of the first of six nonobstructed 24 h kidneys. $^{\dagger}P<0.05$ for Obstr. vs Ctrl. Insert: results are shown of qRT-PCR for mRNA-encoding IL-12 p35 and IL-23 p30 in pooled CD11c-enriched cells from

obstructed kidneys at 24 and 72 h after left UUL. RNA was prepared without overnight culture. Results are expressed as fold expression relative to that of the cell preparations from the nonobstructed kidneys.

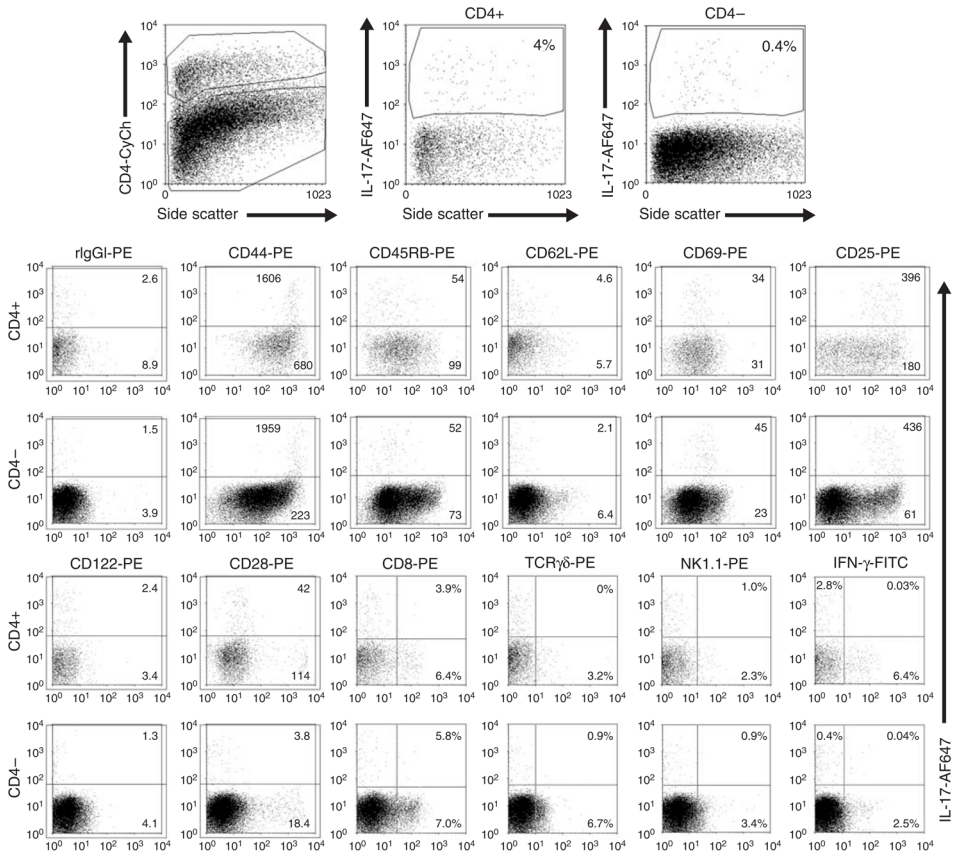

Figure 10. IL-17-competent, CD4$^+$ T cells within acutely obstructed kidneys have the phenotype of activated, memory T cells

Flow cytometric analysis is shown for CD4$^+$ and CD4$^-$ T cells present among a CD45-enriched cell suspension prepared by magnetic bead separation from a pooled digest of three mouse kidneys 72 h after ureteral ligation. The cell suspension was cultured overnight in the presence of 1.0 μg/ml anti-CD3ε stimulatory antibody. A Golgi export inhibitor was added for the final 4 h of culture. Aliquots of cells for each condition were surface stained for CD4 and for a panel of additional T-cell surface markers then intracellularly stained with antibodies against IL-17 (anti-IL-17) and IFNγ (anti-IFNγ). The gating region for CD4$^+$ cells is illustrated in the upper left dot plots. The proportion of cells that were positive for intracellular IL-17 staining is shown for CD4$^+$ and CD4$^-$ populations in the upper right dot plots. The remaining dot plots, gated on either CD4$^+$ or CD4$^-$ populations, demonstrate intracellular staining for IL-17 (*y* axis) and surface staining with PE-coupled antibodies against various T-cell markers or intracellular staining for IFNγ (*x* axis). Numerical values of the median fluorescence intensity or the percentage positive for each PE-labeled surface marker are shown for IL-17$^+$ and IL-17$^-$ cells. In the case of IFNγ staining (lower right), the proportions of cells that are IL-17$^+$/IFNγ^-, IL-17$^+$/IFNγ^+, and IL-17$^-$/IFNγ^+ are indicated (a similar analysis of IFNγ^+ cells among the CD4$^+$ and CD4$^-$ populations is presented in Supplementary Figure S5).

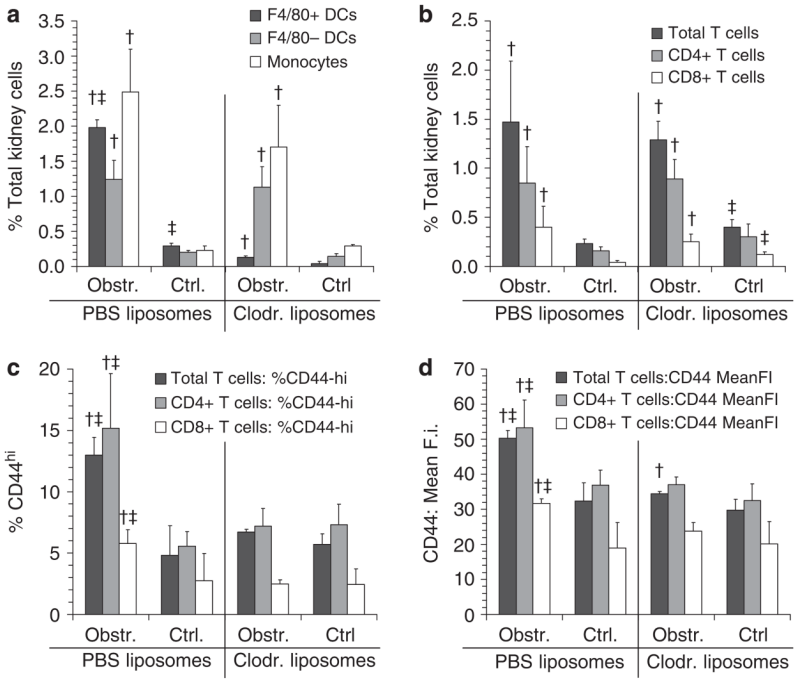

Figure 11. Reduction of F4/80$^+$ DCs is associated with reduced proportion of CD44^{hi} T cells within kidney cell suspensions at 72 h after acute urinary obstruction

Graphical results are shown for surface staining of cell suspensions prepared from obstructed (Obstr.) and nonobstructed (Ctrl.) kidneys 72 h following unilateral (left) ureteral ligation. Groups of mice were pretreated with inert liposomes (PBS, $n = 4$) and clodronate-containing liposomes (Clodr., $n = 4$). (a) The proportions of the total kidney cells suspensions that stained for surface marker combinations indicative of F4/80$^+$ DCs (CD45$^+$/CD11c$^+$/Ly6C$^-$/F4/80$^+$), F4/80$^-$ DCs (CD45$^+$/CD11c$^+$/Ly6C$^-$/F4/80$^-$), and monocytes (CD45$^+$/CD11c$^-$/Ly6C$^+$/F4/80$^-$) are shown as mean±s.d. for each condition. (**b**) The proportions of the total kidney cells suspensions that stained for surface marker combinations indicative of total T cells (CD45$^+$/CD3$^+$), CD4$^+$ T cells (CD45$^+$/CD3$^+$/CD4$^+$), and CD8$^+$ T cells (CD45$^+$/CD3$^+$/CD8$^+$) are shown as mean±s.d. for each condition. (**c**) The proportions of total T cells, CD4$^+$ T cells, and CD8$^+$ T cells that stained highly for CD44 are shown as mean±s.d. for each condition. (**d**) The mean fluorescence intensities for CD44 surface staining of total T cells, CD4$^+$ T cells, and CD8$^+$ T cells are shown as mean±s.d. for each condition. $^\dagger P<0.05$ for Obstr. vs equivalent condition Ctrl. $^\ddagger P<0.05$ for PBS vs equivalent condition for Clodr.